Scanning tunneling microscopy of a stage-1 CuCl$_2$ graphite intercalation compound

C. H. Olk and J. Heremans

Physics Department, General Motors Research Laboratories, Warren, Michigan 48090-9055

M. S. Dresselhaus, J. S. Speck, and J. T. Nicholls

Massachusetts Institute of Technology, Cambridge, Massachusetts 02189

(Received 20 February 1990)

We report a scanning-tunneling-microscope (STM) study of a stage-1 graphite intercalation compound (GIC) of approximate stoichiometry C$_6$CuCl$_2$. When the sample bias is positive with respect to the tip, we observe a hexagonal symmetry in which all the atoms of the graphite surface plane are imaged. This is in contrast to the threefold symmetry usually seen in atomic-resolution STM images of highly oriented pyrolytic graphite (HOPG), which we also observe on a reference sample of HOPG. The threefold symmetry is attributed to the *ABAB* stacking of the atomic layers in HOPG. In GIC's, this stacking sequence is interrupted by the intercalate layer, so that for the stage-1 compound all carbon atoms in the plane become equivalent, and sixfold symmetry develops. When the sample is biased negatively with respect to the tip, we observe a strikingly different STM image for the GIC; we believe that the pattern in this case is mainly due to the intercalate layer and the change in the electronic structure of graphite resulting from the presence of the intercalate layer. We also observe a reduction in the corrugation amplitude, between carbon-atom sites and the centers of the hexagonal nets, on the GIC relative to the HOPG.

INTRODUCTION

The ability of the scanning tunneling microscope (STM, or scanning tunneling microscopy) to probe both geometric and spectroscopic features of surfaces in real space was recognized by its inventors[1] and is now well known.[2] Of the wide variety of materials that have come under investigation by the STM,[3] graphite is one of great interest. Graphite is used extensively to calibrate the piezoelectric constants of the scanners and as a substrate because the surface typically exhibits very large flat areas. Graphite displays a number of unique physical features and has been the subject of many experimental[4-8] and theoretical[9-16] STM studies. The two most notable features of the surface of graphite, as observed by STM, are the threefold (rather than sixfold) symmetry of the STM pattern and the large corrugation amplitude (CA) between the atomic sites and the centers of the hexagons. The former is the result[9] of the *ABAB* stacking sequence of the three-dimensional layered structure, producing two inequivalent atomic sites per planar unit cell. Three of the atoms in a single surface hexagonal net, α sites, lie directly above three atoms in the layer below and are electronically coupled to them. The other three atoms in the surface net, β sites, lie above the centers of the nets below. The origin of the anomalously large corrugation feature often observed[6] with STM of graphite is not fully understood and may be a combination of physical and electronic effects. We address this briefly in the analysis of the data.

Several authors[10,12,14-16] of theoretical work on graphite have suggested that STM images of graphite intercalation compounds (GIC's) would be of great interest and may aid in the general interpretation of topographic and spectroscopic STM data. Although much is known about the bulk electronic and structural properties of GIC's,[17] several questions concerning these compounds, such as the intercalation kinetics and exact charge transfer, remain controversial.[18] Two types of GIC's can be synthesized, donor compounds in which electrons are given up by the intercalate to the graphite, and acceptor compounds in which electrons are transferred from the graphite to the intercalate. Typical donor compounds contain atomic species such as alkali metals, while acceptor compounds are formed from molecular species such as metal chlorides and other Lewis acids. Two STM studies have been performed on acceptor-type GIC's. The first, a study of the GIC's C$_6$FeCl$_3$ and C$_6$BiCs,[19] the second[20] on C$_6$CoCl$_2$. A STM study of the surface structure of the donor intercalation compound LiC$_6$ (Ref. 21) reported images of a surface layer of the intercalate. A more recent STM study[22] of potassium, rubidium, and cesium donor GIC's reported that images of stage-1 compounds contain a periodic surface superlattice exhibiting peaks having 2 times the peak spacing of highly oriented pyrolytic graphic (HOPG), as well as the peaks usually seen on graphite.

STM images are dominated by the spatial dependence of the surface-state wave functions. Depending on the bias of the sample relative to the tip, images can contain peaks in tunneling current from states lying just above or just below the Fermi level. The decay rate of a plane wave into the vacuum and the resultant local density of states have been examined theoretically for samples with defects[16,23] and intercalates.[15,24] Recently, Selloni, Chen, and Tosatti[15] presented a calculation of the tunneling conductance for a donor compound, lithium-intercalated graphite LiC$_6$. The tunneling conductance is assumed to

be proportional to the density of states at the location of the STM tip and at the energy $E = E_F + V$, where E_F is the Fermi level and V the applied voltage between the tip and sample. They found that most differences in the band structure of LiC$_6$ relative to graphite can be explained by a rigid shift which lowers the total density of states by approximately 2 eV. However a splitting of the π^* saddle-point state of graphite into two features for LiC$_6$ was found. These bands appear at about -0.8 and $+0.8$ eV. They calculated the local density of states inside and outside the sample for three different positions on the surface. With the sample bias $+0.8$ V [tip bias negative in Fig. 1(a)], the value of the local electron density of states approximately 2 Å from the surface, and above a site containing a Li atom in the layer below, appears to be somewhat greater than the corresponding local density of states above sites containing a carbon atom. That is to say, electrons may tunnel out of the tip into sites containing Li atoms [see Fig. 1(a)]: thus spatial images of the lithium layer may be visualized through the top graphite layer.

This paper presents experimental evidence of these effects. Unfortunately, donor GIC's are mostly unstable in air, the environment used for our measurements. We therefore report data on an acceptor compound, which is relatively stable in air. A theoretical work on donor and acceptor GIC's by Qin and Kirczenow[24] reported constant-current STM profiles in which the presence of the intercalate is felt only through its influence on the average potential energy of an electron (hole) in the graphite layer and on the number of electrons (holes) present. This theory predicts that there should be no carbon-atom asymmetry, even when the stacking sequence of the graphite layers close to the surface is AB, as in a stage-2 GIC. Since this treatment omitted the effects of the in-plane periodicity of the intercalate, which clearly influence our images, we therefore extracted arguments from both Qin and Kirczenow[24] and Selloni et al.[15] to reach the picture for acceptor compounds presented here. The reduction in corrugation amplitude (CA) that we have observed upon intercalation of acceptor species qualitatively agrees with the calculated reduction of CA found in the model of Qin and Kirczenow.[24]

EXPERIMENT

We have taken STM images of the first-stage acceptor compound CuCl$_2$-GIC (with approximate stoichiometry C$_6$CuCl$_2$), so that the graphite layers are separated from one another by a single layer of the CuCl$_2$ intercalate. The sample was prepared by high-temperature intercalation of HOPG with CuCl$_2$ under Cl$_2$ overpressure, then charac-

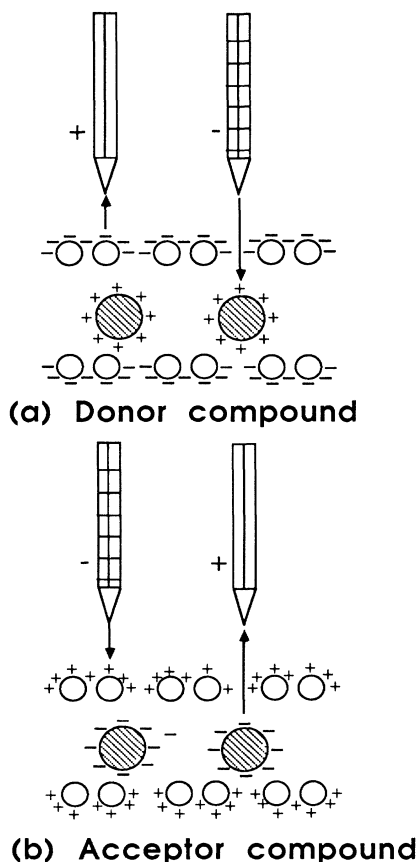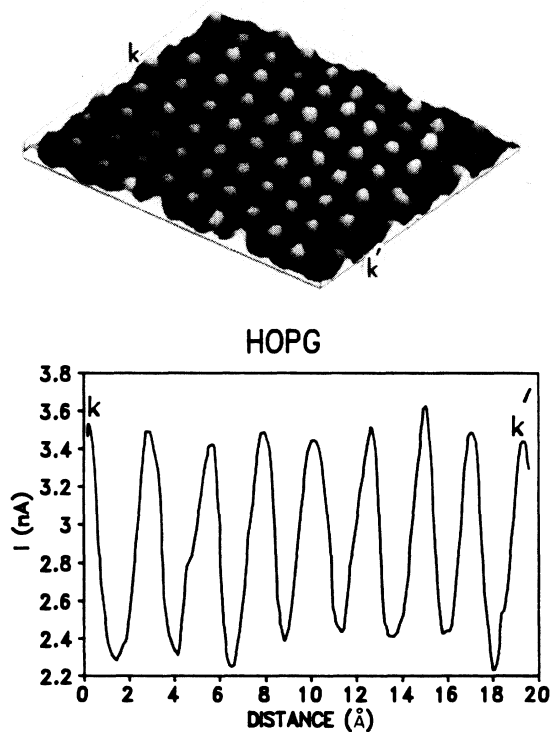**(a) Donor compound**

(b) Acceptor compound

FIG. 1. Schematic diagram of the tunneling sites and direction of the electrons for (a) a donor and (b) an acceptor graphite intercalation compound. The charge transfer associated with each compound is indicated schematically.

HOPG

FIG. 2. A 20.75×20.75-Å^2 atomic-resolution STM image, taken in the current-imaging mode, of the surface of HOPG showing trigonal symmetry. Below is a cross section detailing the atomic separation and the corrugation amplitude. The cross section is taken along a line that connects points k and k'. The atomic separation is 2.45 Å.

terized by x-ray diffraction to determine the stage and other structural parameters of the superlattice.[25] A Raman spectrum was taken on the freshly cleaved sample shortly before mounting it in the STM, to verify that the sample was indeed stage 1. Obviously, the Raman scattering occurs over a much greater depth (1000 Å) than is imaged by STM, and the STM structures we will describe are not necessarily consistent with those in the bulk of the GIC. The results presented below were reproduced upon cleaving the GIC sample while it was mounted in the STM.

Our microscope is "home-built" and has a rigid design with stacked plates and an air table for vibration isolation. The microscope uses a "tube scanner": the scanner is a hollow cylinder of piezoelectric material with five electrodes—four electrodes in quadrants on the outer edge, and one electrode in the middle. The tips are electrochemically etched tungsten wires. The feedback electronics are digital[26] and computer controlled. The acceptor GIC was mounted alongside a freshly cleaved sample of HOPG, so that both samples could be imaged using the same tip under similar conditions. All experiments were done in air at room temperature. Images were taken in the "constant-height mode": the feedback control which maintains a constant tunneling current by adapting the z displacement of the piezoelectric material was

only used during the approach. Once a stable tunneling current was achieved, and before the X-Y scan was initiated, the feedback loop was disconnected. A rapid X-Y scan was then initiated and the variation in tunneling current (nA) was monitored and constitutes the z axis of our images. Because of the minimal thermal drift of the instrument, it was possible to obtain atomic resolution images.

For reference purposes, images of HOPG were taken prior to and following those taken on the GIC. One such image, which can be obtained independent of polarity, is shown in Fig. 2. It displays the trigonal symmetry of the β atomic sites[9] in the surface layer of bulk graphite. The measured cross section yields an atomic separation of 2.45 ± 0.05 Å; the accepted crystallographic value is 2.46 Å.

Images of the acceptor GIC at negative sample bias with respect to the tip are shown in Fig. 3. When the sample bias is positive with respect to the tip, we record the images shown in Fig. 4. We used the same tip for measurement on the HOPG and on the intercalated sample. Since the images of the HOPG taken after those of the GIC also display atomic resolution with threefold symmetry, we believe that the images of the GIC are not due to "multiple-tip" effects.
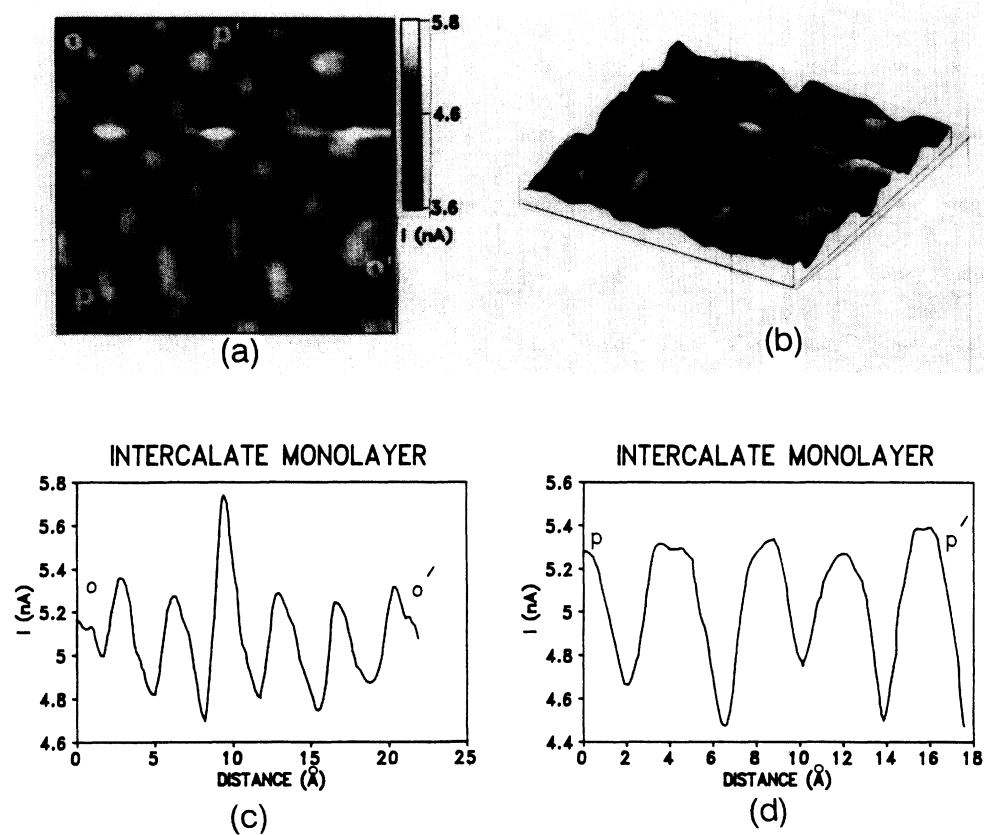

(a)

(b)

INTERCALATE MONOLAYER

INTERCALATE MONOLAYER

(c)

(d)

FIG. 3. STM image of the intercalate $CuCl_2$ layer lying just below the surface graphite monolayer. (a) A gray-scale image, and (b) a three-dimensional projection. The cross sections, taken along lines that connect the points indicated within image (a), are labeled and shown in the graphs of (c) and (d). The sample bias is -0.01 V, the image size is 20.75×20.75 Å^2. The imaged objects show as a unit cell a two-dimensional parallelogram with sides $a=3.5\pm0.2$ Å and $b=3.9\pm0.2$ Å, with an angle of 121° between them.
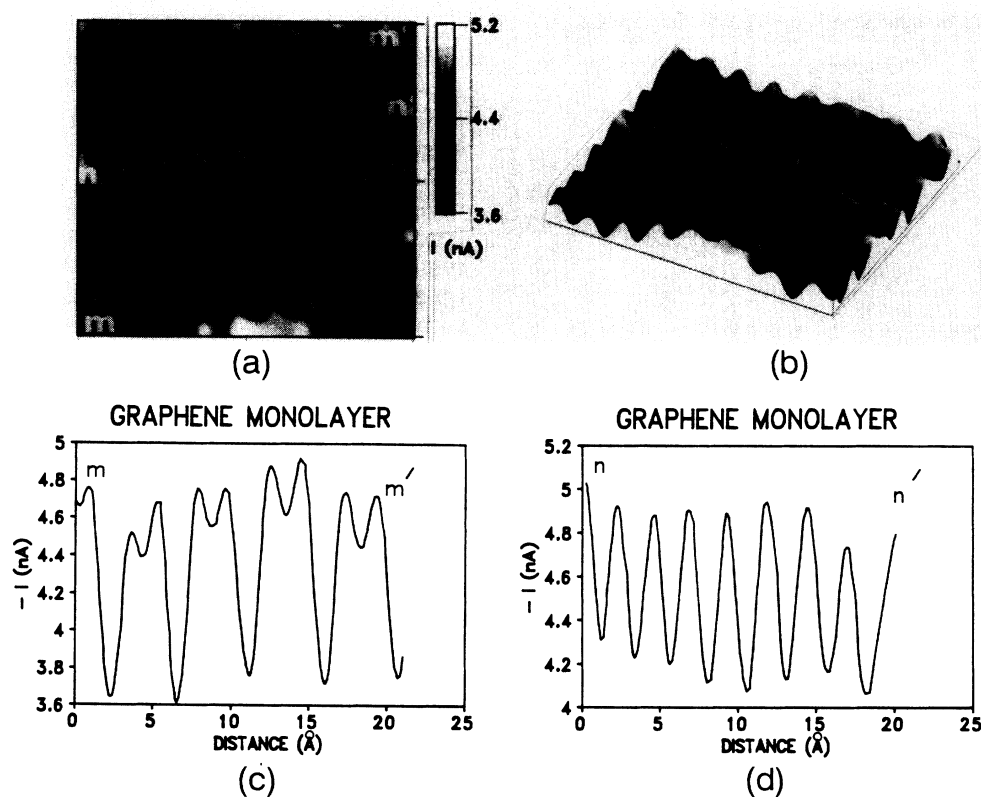
FIG. 4. A 20.75×20.75-Å^2 STM image of the graphene monolayer of the acceptor compound taken with a sample bias voltage of +0.01 V. All six atoms are clearly revealed. (a) A grey scale image, (b) a three-dimensional projection, (c) a cross section, taken along lines that connect the points indicated within image (a), showing the nearest-neighbor atoms separated by the holes of the hexagonal net, and (d) a cross-section through the β sites.

ANALYSIS

Figure 3(a) is a STM image of the acceptor compound with the sample bias −0.01 V. This image reveals rows of aligned structures. Figure 3(b) shows a three-dimensional (3D) plot of the tunneling current versus x and y displacements for this layer. The imaged objects form a two-dimensional parallelogram with sides $a = 3.5 \pm 0.2$ Å and $b = 3.9 \pm 0.2$ Å with an angle of 121° between them. These dimensions were taken from the cross sections shown in Figs. 3(c) and 3(d).

In the acceptor compound, electrons are given by the graphite layers to the $CuCl_2$ molecules. Inverting the analysis by Selloni et al.,[15] we expect that for a negative sample bias the value of the local electron density of states due to the presence of the $CuCl_2$ molecules, in the layer below, can be greater than the local density of states of the surface layer containing carbon atoms. This case is shown schematically in Fig. 1(b), with the tip bias positive over the acceptor compound, in which electrons are shown tunneling out of a site (state) containing a $CuCl_2$ molecule in the layer below. We therefore believe that the imaged structures we see in Fig. 3(a) are predominantly due to $CuCl_2$ molecules. The in-plane density of these molecules relative to that of carbon atoms, for the same area (see Fig. 4), supports our belief.

According to Fig. 3(a) the $CuCl_2$ intercalate forms a monoclinic lattice between the graphene layers which

projects into the parallelogram described. Speck[25] used x-ray studies to determine that the $CuCl_2$ between the graphite layers of this GIC forms a lattice with an equiaxed oblique unit cell with sides $a = b = 3.81$ Å and an angle $\gamma = 128°$. The unit cell we see in Fig. 3 is also oblique, with $a \neq b$, and the angle we measure is somewhat different (121°), but γ is still compatible with the results of Speck[25] because of the angular distortion that our system induces on the images during scanning. In part, these differences could be due to the fact that we measure a layer of $CuCl_2$ that is very close to the top surface. We have also obtained images, on other areas of the sample, of other periodic structures that exhibit sharp boundaries, but they are probably $CuCl_2$ molecules adsorbed on the top surface, since those images were independent of the sign of the bias voltage. The image shown in Fig. 3 could only be obtained with the sample biased negatively.

In Fig. 4(a) we show a 20.75×20.75 Å^2 image of the surface of the GIC with the sample bias +0.01 V. Figure 4 was taken at the same physical location as Fig. 3, with only the sign of the bias voltage changed during tunneling. Thermal drift of the imaged area was small. The images in Fig. 4 clearly reveal the hexagonal surface structure of graphite including all six carbon atoms per net. In Table I we report the various dimensions measured on Fig. 4: the distance between nearest-neighbor atoms, the diameter of the hexagons, and the β to β site separation. These values are in good agreement with the accepted

TABLE I. Site-site distances and corrugation amplitudes (in Å).

Distance	"Graphene" Expt.	HOPG Accepted[a]	Diff. (%)
Carbon-Carbon	1.50±0.03	1.42	+5.6
Diameter	2.73±0.06	2.84	−3.8
β-site–β-site	2.42±0.05	2.46	−1.6
Corrugation	$CuCl_2$-GIC	HOPG	Diff. (%)
$\frac{1}{2}$ β-site–β-site	0.10±0.02	0.28±0.02	−64.3
β-site–center	0.13±0.02	0.28±0.02	−53.6

[a]Reference 17.

values for pristine graphite, also given in Table I. We therefore interpret the image in Fig. 4(a) to be that of the top graphene plane of the GIC. Under these bias conditions, electrons are tunneling into states (sites) made available in the graphene surface monolayer by the transfer of charge to the intercalate. This is shown schematically in Fig. 1(b) for the acceptor compound with negative tip bias.

STM images of graphite planes on bulk graphite, as shown in Fig. 2, display the carbon atoms arranged with trigonal symmetry. The picture in Fig. 4(a) shows hexagonal symmetry. The insertion of the $CuCl_2$ molecules between each pair of graphene layers increases the host-layer separation to 9.40 Å. The stacking sequence of the graphene planes becomes AA,[25] and the intercalate and graphene layers are incommensurate. Thus all carbon-atom sites become equivalent and all six carbon atoms in the hexagonal net appear in STM images. Since Figs. 3 and 4 are taken at the same location, we can superimpose them, and conclude that we see no registry between the carbon atoms and the $CuCl_2$ molecules on adjacent layers. Furthermore, no preferential alignment is found between the $CuCl_2$ rows and any ⟨110⟩ axis of the graphene planes as reported by Speck and others.[17,25] One possible explanation for this discrepancy is that the STM images represent only the uppermost $CuCl_2$ layer, which might be different from the $CuCl_2$ layers in the bulk of the sample.

An issue in the interpretation of STM images is the origin of the large CA of the atomic sites seen on several layered materials including graphite. A variety of explanations,[5,6,9-11,13] such as tip-contamination effects, elastic deformation of the surface due to atomic forces between the tip and the sample, and the amplitude of the electronic wave functions at the point where the signal is measured, have been put forth to account for the observed corrugations. The following CA's are given for a relative comparison, since absolute values would have to be calculated using the actual barrier height for this GIC. In the absence of such a direct measurement, we used the effective barrier-height value for a tungsten tip and graphite surface.

The corrugation amplitude, calculated from the measured tunneling current observed on an image of HOPG taken under the same bias and current conditions used to acquire the image in Fig. 4, is 0.28±0.02 Å when measured from the β sites to the center of the hexagons. This value agrees well with the hard-sphere estimate of

0.21–0.29 Å obtained from helium-scattering experiments.[27] By comparison (see Fig. 5 and Table I), the corrugation of the same sites of our GIC surface monolayer is 0.13±0.02 Å [see Fig. 4(d)], the HOPG CA being larger by more than a factor of 2 (see Table I).

Although giant CA's (≫1 Å) have not been observed using the current-imaging mode, CA's 4–6 times the hard-sphere estimate have been reported.[6,28] If we assume that at the separation distance used in our scans the tip and the sample surface are in a repulsive regime and an initial elastic deformation of the surface is maintained during the scanning of an image, decreases in the c-axis (z direction) compressibility of the GIC, relative to that of HOPG, may lead to proportional decreases in the CA. The c-axis compressibility has been measured for a stage-1 $CoCl_2$ GIC (Ref. 29) and for graphite[30] to be 1.1±0.5 and 2.9±0.3 ($\times 10^{-3}$ kbar^{-1}), respectively.[31] In this connection, it is interesting to note that the decrease in compressibility of HOPG by 62.1% through intercalation with $CuCl_2$ is remarkably close to the 64.3% decrease in CA that we measure in the GIC relative to HOPG.

The transfer of charge, from the "graphene" surface layer to the layer of intercalate below, may electronically alter the total charge density in a manner that reduces the CA. Our value of CA measured on HOPG is very near the value predicted by Selloni[11] from calculated valence charge density. Upon careful examination of the image of the graphene layer, increases in image brightness at and near the positions of several carbon atoms and carbon-carbon bonds becomes apparent. When the images of Figs. 3 and 4 are superimposed, we find that the intercalate molecules lie predominantly centered below these high-brightness positions in the graphene layer. The charge, and therefore the availability of tunneling states in the graphene layer, is modulated by the location of the intercalate in the layer below. Thus the CA is sensitive to electronic effects, specifically the amount and distribution of charge transfer between the guest and host near the surface. This is in agreement with the theoretical findings of Qin and Kirczenow.[24]

A STM investigation of three donor GIC's by Kelty and Lieber[22] found a surface structure that exhibits peak spacings that match the in-plane periodicity of the inter-
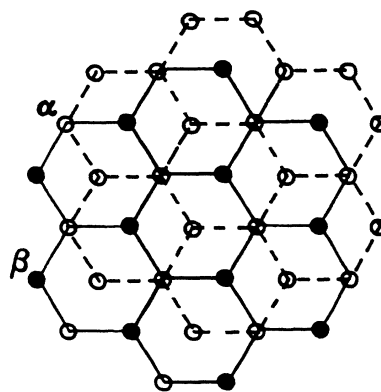

FIG. 5. Geometry of graphite, showing α and β sites.

calate in the bulk. Although theoretical predictions for stage-1 (Refs 9 and 14) and stage-2 (Ref. 24) GIC's indicate that all of the surface carbon sites should be observed by STM, they were not in these donor studies.[21,22] In contrast, in the stage-1 $CuCl_2$-GIC, we do observe all the atoms of the graphene surface monolayer, but our results also reveal local modulations in the distribution of surface charge. Unlike the present study, the images obtained on the donors[21,22] were found to be independent of the sign of the bias voltage. This indicates that the spatial location of surface sites imaged on the donor compounds contain both filled and empty states near the Fermi energy. In a donor GIC the relatively large charge transfer, together with the commensurate structure, should lead to a much more pronounced modulation of the graphene surface structure than that for the low charge-transfer incommensurate acceptor GIC of the present study.

The first reported STM study performed on acceptor-type GIC's (Ref. 19) did not reveal surface structures significantly different from those found by STM of HOPG. A second study[20] on an acceptor GIC reported only a shift of the Fermi level acquired through scanning tunneling spectroscopy, and did not include any images of the GIC.

Finally, we believe that we give strong supporting evidence that the inequivalency of the α and β sites in STM images of graphite is due to preferential interlayer coupling, and that once that coupling is removed (as, for example, by incommensurate intercalation) all carbon atoms of the surface layer are imaged. Our results further suggest that the corrugation amplitude is due to both electronic and elastic effects between the tip and the sample surface. It will be of further interest to study nonuniform charge-distribution effects in the metal chloride acceptor GIC's over a somewhat larger area.

ACKNOWLEDGMENTS

[1]G. Binnig and H. Rohrer, Rev. Mod. Phys. **59**, 615 (1987).

[2]P. K. Hansma and J. Tersoff, J. Appl. Phys. **61**, 2 (1987).

[3]R. M. Feenstra (unpublished).

[4]S. Park and C. F. Quate, Appl. Phys. Lett. **48**, 2 (1986).

[5]J. M. Soler, A. M. Baro, N. Garcia, and H. Rohrer, Phys. Rev. Lett. **57**, 444 (1986).

[6]H. J. Mamin, E. Ganz, D. W. Abraham, R. E. Thomson, and J. Clarke, Phys. Rev. B **34**, 9015 (1986).

[7]J. Schneir, R. Sonnenfeld, P. K. Hansma, and J. Tersoff, Phys. Rev. B **34**, 4979 (1986).

[8]A. Bryant, D. P. E. Smith, and C. F. Quate, Appl. Phys. Lett. **48**, 834 (1986).

[9]I. P. Batra, N. Garcia, H. Rohrer, H. Salemink, E. Stoll, and S. Ciraci, Surf. Sci. **181**, 126 (1987).

[10]J. Tersoff, Phys. Rev. Lett. **57**, 440 (1986).

[11]A. Selloni, P. Carnevali, E. Tosatti, and C. D. Chen, Phys. Rev. B **31**, 2602 (1985).

[12]H. A. Mizes, S. Park, and W. A. Harrison, Phys. Rev. B **36**, 4491 (1987).

[13]S. Ciraci and I. P. Batra, Phys. Rev. B **36**, 6194 (1987).

[14]D. Tománek and S. G. Louie, Phys. Rev. B **37**, 8327 (1988).

[15]A. Selloni, C. D. Chen, and E. Tosatti, Phys. Scr. **38**, 297 (1988).

[16]H. A. Mizes and W. A. Harrison, J. Vac. Sci. Technol. A **6**, 300 (1988).

[17]M. S. Dresselhaus, *Intercalation in Layered Materials* (Plenum, New York, 1986).

[18]M. S. Dresselhaus, Mater. Sci. Eng. B **1**, 259 (1988).

[19]S. Gauthier, S. Rousset, J. Klein, W. Sacks, and M. Belin, J. Vac. Sci. Technol. A **6**, 360 (1988).

[20]M. Tanaka, W. Mizutani, T. Nakashizu, N. Morita, S. Yamazaki, H. Bando, M. Ono, and K. Kajimura, J. Microsc. (Oxford) **152**, 183 (1988).

[21]D. Anselmetti, R. Wiesendanger, and H. J. Güntherodt, Phys. Rev. B **39**, 11 135 (1989).

[22]S. P. Kelty and C. M. Lieber, Phys. Rev. B **40**, 5856 (1989).

[23]R. J. Hamers, J. Vac. Sci. Technol. B **6**, 1462 (1988).

[24]X. Qin and G. Kirczenow, Phys. Rev. B **39**, 6245 (1989).

[25]J. S. Speck, Ph.D. thesis, Massachusetts Institute of Technology, 1989.

[26]Atomis, Inc. (Berkeley, CA)/McAllister Technical Services (Berkeley, CA).
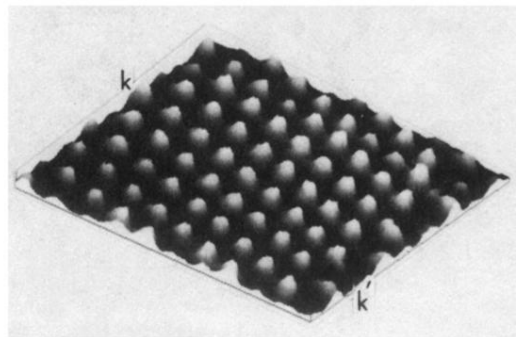
[27]G. Boata, P. Cantini, and R. Tatarek, Phys. Rev. Lett. **40**, 887 (1978).

[28]S. Morita, S. Tsukada, and N. Mikoshiba, J. Vac. Sci. Technol. A **6**, 354 (1988).

[29]J. T. Nicholls, C. Murayama, H. Takahashi, N. Mōri, T. Tamegai, Y. Iye, and G. Dresselhaus, Phys. Rev. B **41**, 4953 (1990).

[30]Y. Iye, O. Takahashi, S. Tanuma, K. Tsuji, and S. Minomura, J. Phys. Soc. Jpn. **51**, 475 (1982).

[31]Because of the structural similarity between stage-1 $CoCl_2$-GIC and stage-1 $CuCl_2$-GIC, it is expected that the compressibility of the two compounds should also be similar. We have therefore used the compressibility data of the former in place of the latter, which has not yet been reported.
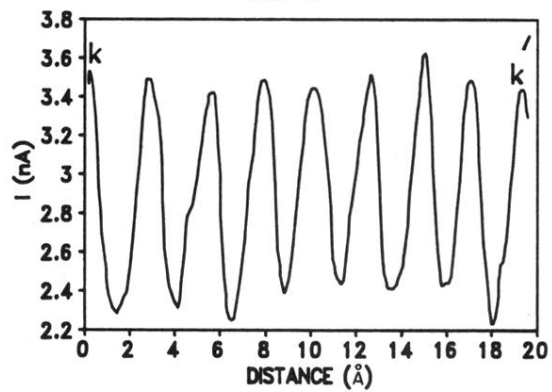
FIG. 2. A 20.75×20.75-Å^2 atomic-resolution STM image, taken in the current-imaging mode, of the surface of HOPG showing trigonal symmetry. Below is a cross section detailing the atomic separation and the corrugation amplitude. The cross section is taken along a line that connects points k and k'. The atomic separation is 2.45 Å.
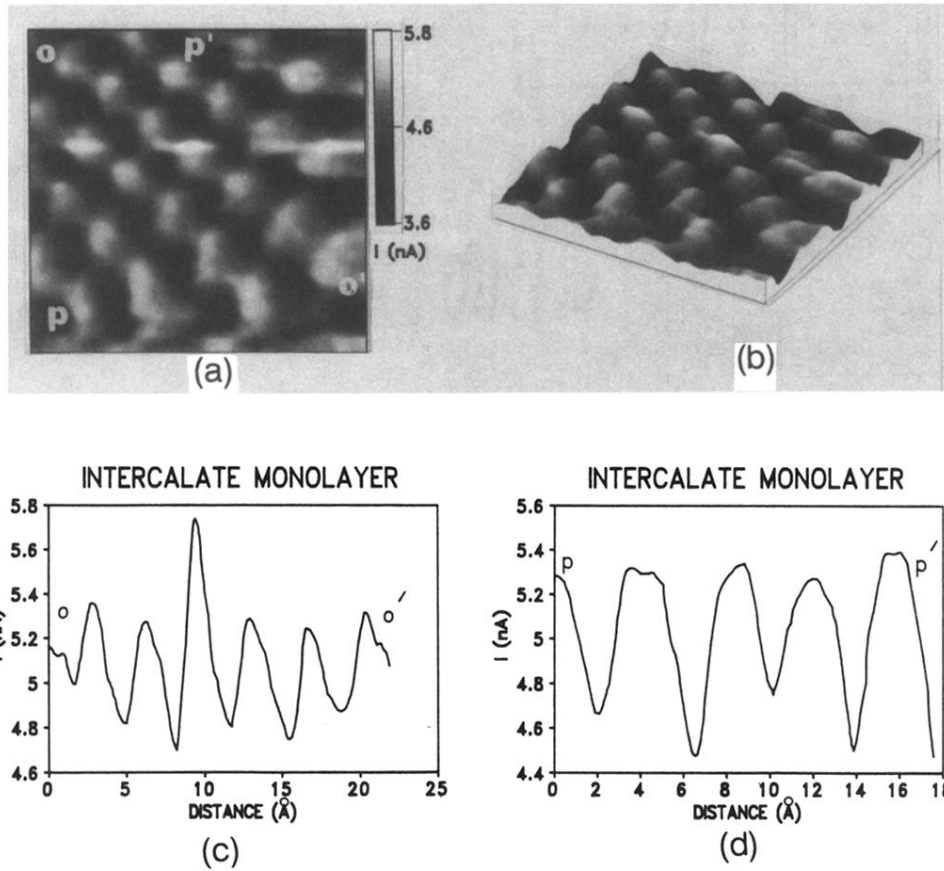
FIG. 3. STM image of the intercalate $CuCl_2$ layer lying just below the surface graphite monolayer. (a) A gray-scale image, and (b) a three-dimensional projection. The cross sections, taken along lines that connect the points indicated within image (a), are labeled and shown in the graphs of (c) and (d). The sample bias is -0.01 V, the image size is 20.75×20.75 Å^2. The imaged objects show as a unit cell a two-dimensional parallelogram with sides $a = 3.5 \pm 0.2$ Å and $b = 3.9 \pm 0.2$ Å, with an angle of 121° between them.
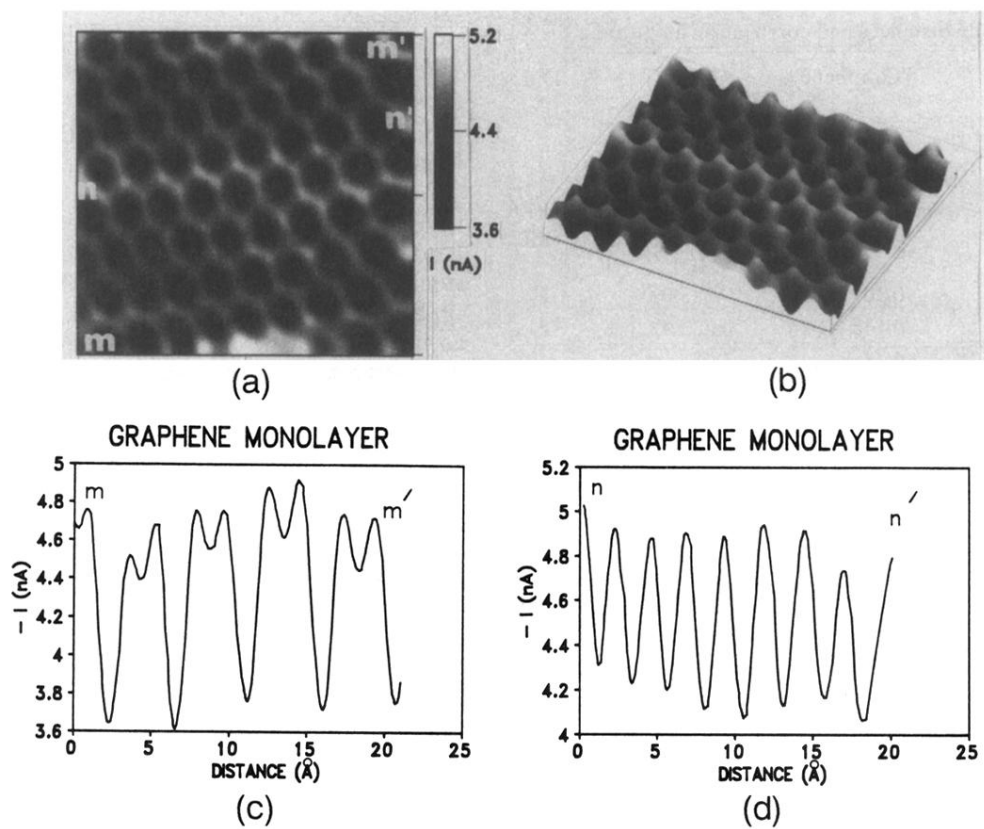
FIG. 4. A 20.75×20.75-Å^2 STM image of the graphene monolayer of the acceptor compound taken with a sample bias voltage of $+0.01$ V. All six atoms are clearly revealed. (a) A grey scale image, (b) a three-dimensional projection, (c) a cross section, taken along lines that connect the points indicated within image (a), showing the nearest-neighbor atoms separated by the holes of the hexagonal net, and (d) a cross-section through the β sites.